LETTERS

Listeriolysin O allows *Listeria monocytogenes* replication in macrophage vacuoles

Cheryl L. Birmingham[1,2], Veronica Canadien[1], Natalia A. Kaniuk[1], Benjamin E. Steinberg[1,3], Darren E. Higgins[4] & John H. Brumell[1,2,3]

***Listeria monocytogenes* is an intracellular bacterial pathogen that replicates rapidly in the cytosol of host cells during acute infection[1]. Surprisingly, these bacteria were found to occupy vacuoles in liver granuloma macrophages during persistent infection of severe combined immunodeficient (SCID) mice[2]. Here we show that *L. monocytogenes* can replicate in vacuoles within macrophages. In livers of SCID mice infected for 21 days, we observed bacteria in large LAMP1$^+$ compartments that we termed spacious *Listeria*-containing phagosomes (SLAPs). SLAPs were also observed *in vitro*, and were found to be non-acidic and non-degradative compartments that are generated in an autophagy-dependent manner. The replication rate of bacteria in SLAPs was found to be reduced compared to the rate of those in the cytosol. Listeriolysin O (LLO, encoded by *hly*), a pore-forming toxin essential for *L. monocytogenes* virulence[1], was necessary and sufficient for SLAP formation. A *L. monocytogenes* mutant with low LLO expression was impaired for phagosome escape but replicated slowly in SLAPs over a 72 h period. Therefore, our studies reveal a role for LLO in promoting *L. monocytogenes* replication in vacuoles and suggest a mechanism by which this pathogen can establish persistent infection in host macrophages.**

L. monocytogenes is a Gram-positive bacterial pathogen that causes acute infection in immunocompromised individuals and pregnant women[1]. After entry into host cells, this pathogen initially occupies a phagosome. LLO, a cholesterol-dependent pore-forming toxin[3], blocks phagosome–lysosome fusion by generating small pores that uncouple pH and calcium gradients across the phagosome membrane[4]. A second function for LLO, in concert with the action of two phospholipases, is to promote phagosome escape by the bacteria[1]. Once within the cytosol, *L. monocytogenes* replicates rapidly and usurps the host actin polymerization machinery to move through the cytosol and spread into neighbouring cells[1]. LLO is essential for virulence in animal models of infection[1] and its function is known to be impaired by host innate immune defences[5,6]. LLO is also a major antigen for adaptive immune responses, which normally mediate clearance of *L. monocytogenes* infection[7].

In severe combined immunodeficient (SCID) mice, which lack adaptive immunity, *L. monocytogenes* can cause persistent infection[2]. In these mice, bacteria are localized to macrophages in tissue granulomas (particularly within the liver) and are largely absent from other cell types[2]. Surprisingly, *L. monocytogenes* occupy vacuoles during persistent infection, although the nature of these compartments is unclear (Fig. 1a)[2]. To characterize *Listeria*-containing vacuoles in host cells during persistent infection, we analysed liver sections from SCID mice that had been infected with wild-type *L. monocytogenes* for 21 days. The vacuoles containing bacteria were labelled with lysosomal-associated membrane protein 1 (LAMP1; Fig. 1b, c), indicating that these are endocytic compartments. In agreement with previous findings[2], ~86% of bacteria within the liver sections were found in LAMP1$^+$ vacuoles (Fig. 1c). Approximately half of the *L. monocytogenes*-containing vacuoles were large (up to 7 μm in diameter), with only limited internal membranes (Fig. 1a, c). Therefore, we termed these compartments spacious *Listeria*-containing phagosomes (SLAPs). SLAPs often contained multiple intact bacteria, indicating that bacterial replication was occurring in these compartments.

SLAP formation was also observed *in vitro* after *L. monocytogenes* infection of RAW 264.7 macrophages (Fig. 2a), J774 macrophages (data not shown) and primary bone-marrow derived macrophages (Supplementary Fig. 1). We used RAW 264.7 macrophages for the remainder of our *in vitro* studies. Although most *L. monocytogenes* escaped phagosomes and grew rapidly in the cytosol of RAW 264.7 macrophages as described previously[1], we consistently observed a population of intracellular bacteria within vacuoles. The small percentage of intracellular bacteria that localized to SLAPs (~13% by 4 h post infection) was easily masked by robust replication of cytosolic bacteria and was difficult to observe without vacuolar markers. However, ~46% of infected cells formed SLAPs by this time in infection (Supplementary Fig. 2), and these structures were morphologically indistinguishable from the bacteria-containing compartments formed during persistent infection *in vivo*. Therefore, to gain further insight into the possible mechanisms governing persistent infection by *L. monocytogenes*, we further characterized the SLAP phenotype *in vitro*.

SLAPs often contained multiple intact bacteria (Fig. 2a) and colocalized with LAMP1 (Fig. 2b), similar to those observed in SCID mice. SLAPs also labelled with the autophagy marker LC3 (Fig. 2b, c), suggesting a role for autophagy in the formation of these compartments. Most SLAPs did not contain the lysosomal enzyme cathepsin D. In contrast, significant amounts of cathepsin D were observed in phagosomes containing bacteria killed with paraformaldehyde (PFA; Fig. 2d, e). These observations indicate that viable *L. monocytogenes* block SLAP maturation into degradative phagolysosomes.

L. monocytogenes within SLAPs often exhibited septa (Fig. 2a, arrow), and the number of bacteria within these compartments increased over time (Fig. 2a, f). This increase in bacterial number within SLAPs was independent of cell-to-cell spread (because it also occurred with non-motile *actA* mutant bacteria) and required bacterial protein synthesis (Fig. 2f). These data suggest that bacteria replicate within SLAPs. To test this further, we stained *L. monocytogenes*-infected macrophages with bromodeoxyuridine (BrdU)—a thymidine analogue that is incorporated into replicating DNA. As shown in Fig. 2g and h, SLAPs often contained actively replicating bacteria that labelled with BrdU. It is possible that bacteria

[1]Cell Biology Program, Hospital for Sick Children, Toronto, Ontario M5G 1X8, Canada. [2]Department of Molecular Genetics, [3]Institute of Medical Science, University of Toronto, Toronto, Ontario M5S 1A8, Canada. [4]Department of Microbiology and Molecular Genetics, Harvard Medical School, Boston, Massachusetts 02115-6092, USA.

enter SLAPs after replication in the cytosol. However, non-motile *actA* mutant bacteria within SLAPs did not label with ubiquitin, which normally occurs when these bacteria are exposed to the cytosol[8] (Supplementary Fig. 3a). Also, monomeric red fluorescent protein expressed in the cytosol was not observed within SLAPs (Supplementary Fig. 3b), indicating that cytosolic contents are not delivered to these structures. Therefore, it seems that bacteria within SLAPs are not delivered from the cytosol, but may arise from a viable population that does not escape from the primary phagosome. Multiple bacteria-containing phagosomes may fuse together to form SLAPs. However, treatment of cells with either cytochalasin D or

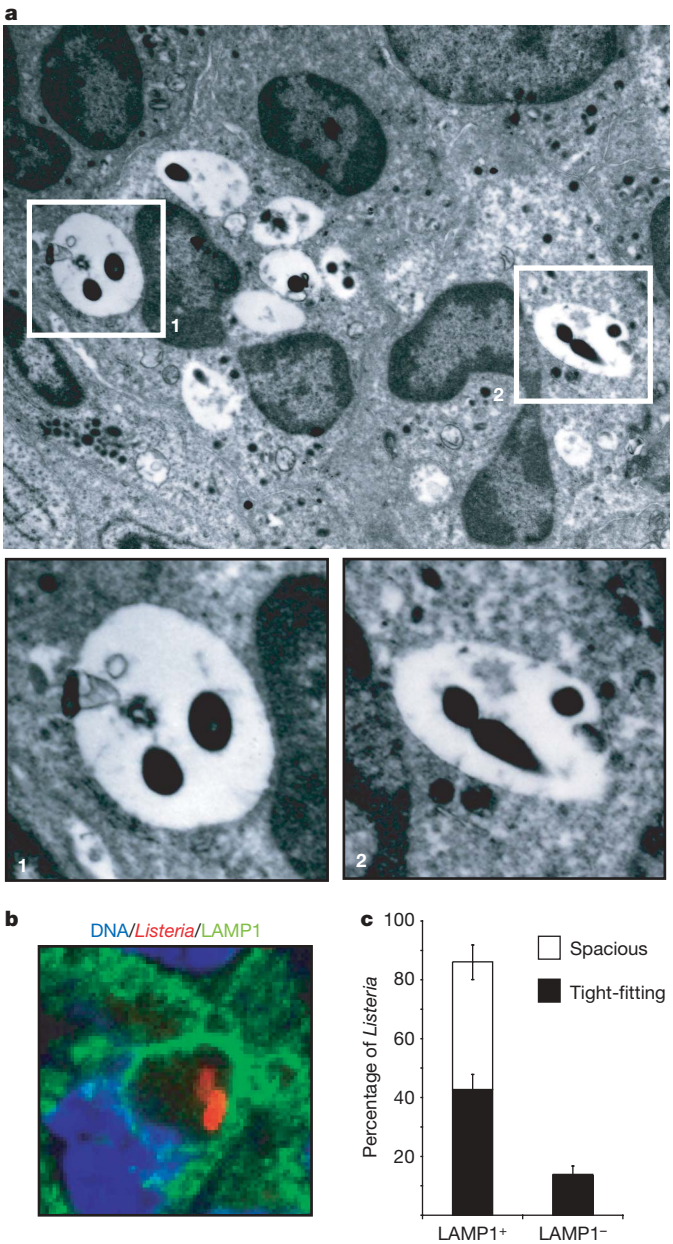

Figure 1 | *L. monocytogenes* colonize SLAPs during chronic infection of SCID mice. **a**, Mice were infected for 21 days and liver granulomas analysed by transmission electron microscopy (TEM). Shown are spacious vacuoles (SLAPs) containing multiple bacteria. Magnification, ×5,200. Region 1 and 2 (white boxes) are enlarged in the lower panels. **b**, SCID mice were infected as in **a** and liver sections stained for LAMP1 (green), bacteria (red) and DNA (blue). Shown is a LAMP1$^+$ SLAP. **c**, The percentage of bacteria in LAMP1$^+$ compartments was quantified and characterized as either spacious or tight-fitting. Mean ± s.e.m. for three mice examined. The image in **a** (from ref. 2) and the tissue sections were provided by E. Unanue.

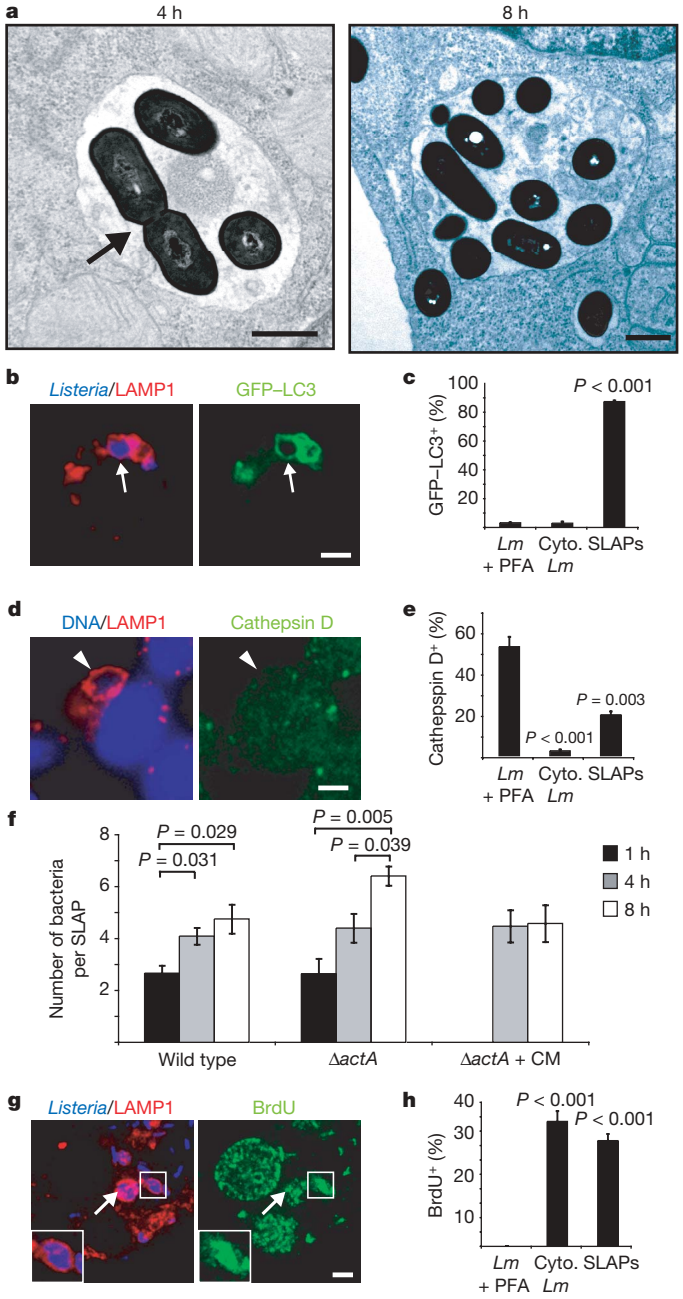

Figure 2 | *L. monocytogenes* replicate slowly in SLAPs during *in vitro* infection of macrophages. **a**, RAW 264.7 macrophages infected for 4 or 8 h were analysed by TEM. Shown are spacious vacuoles (SLAPs) containing multiple bacteria. The arrow indicates septum of dividing bacteria. Scale bars, 0.5 μm. **b**, The arrow indicates a LAMP1$^+$ SLAP colocalizing with green fluorescent protein (GFP)–LC3 in cells infected for 4 h. **d**, The arrowhead indicates a LAMP1$^+$ SLAP devoid of cathepsin D in cells infected for 4 h. Scale bars, 5 μm. **c**, **e**, The percentage of GFP–LC3$^+$ (**c**) or cathepsin D$^+$ (**e**) SLAPs was quantified, and compared to GFP–LC3 or cathepsin D colocalization with cytosolic (Cyto.) bacteria (actin$^+$ or LAMP1$^-$) or PFA-killed bacteria in phagosomes (LAMP1$^+$). Mean ± s.e.m. for three independent experiments. *P* values for conditions significantly different from PFA-killed bacteria are shown. **f**, GFP–LC3-transfected macrophages were infected with wild-type or Δ*actA* bacteria. Where indicated, chloramphenicol (CM) was added to the media at 3 h post infection. The number of bacteria per SLAP was quantified. Brackets indicate significant differences, and corresponding *P* values are shown. **g**, Macrophages were infected with wild-type bacteria for 7 h, pulsed with BrdU for 1 h, and stained for LAMP1 (red), bacteria (blue) and BrdU (green). Magnified images and the arrow indicate SLAPs containing actively replicating bacteria (BrdU$^+$). **h**, The percentage of BrdU$^+$ bacteria in SLAPs, compared to cytosolic and PFA-killed bacteria, was quantified as in **c**.

nocodazole—inhibitors that disrupt the actin and microtubule cytoskeletons, respectively, and thus impair membrane traffic—did not affect the number of bacteria within SLAPs (Supplementary Fig. 3c). Therefore, our data are consistent with bacterial replication within SLAPs.

SLAP formation required continuous bacterial protein synthesis (Supplementary Fig. 2). Therefore, we tested for bacterial virulence factors involved in the formation of these structures. PrfA is a main transcriptional regulator of virulence genes in *L. monocytogenes*[9]. A *prfA* mutant did not form SLAPs (Fig. 3a). An *hly*-deletion mutant, which does not express LLO, also did not form SLAPs, indicating that LLO is necessary for the formation of these compartments (Fig. 3a). Two bacterial phospholipase Cs (PLCs) encoded by *plcA* and *plcB* assist LLO in mediating bacterial escape from the phagosome[1]. However, bacterial mutants of these genes had only minor defects in SLAP formation. *hly* expression in a *prfA* mutant (Δ*prfA* + *hly*) rescued SLAP formation, indicating that LLO is sufficient for the formation of SLAPs (Fig. 3a). LLO was expressed within SLAPs, as shown by specific staining with monoclonal antibodies (Fig. 3b). Therefore, a localized effect of LLO on the vacuole seems to allow bacterial replication within SLAPs.

LLO is known to uncouple pH gradients of the primary phagosome by creating small pores in the phagosomal membrane[10]. This is thought to allow a window of opportunity for LLO- and PLC-mediated lysis of the phagosome, as well as bacterial escape into the cytosol[10]. Because LLO was both sufficient and necessary for SLAP formation and was acting within SLAPs, we hypothesized that

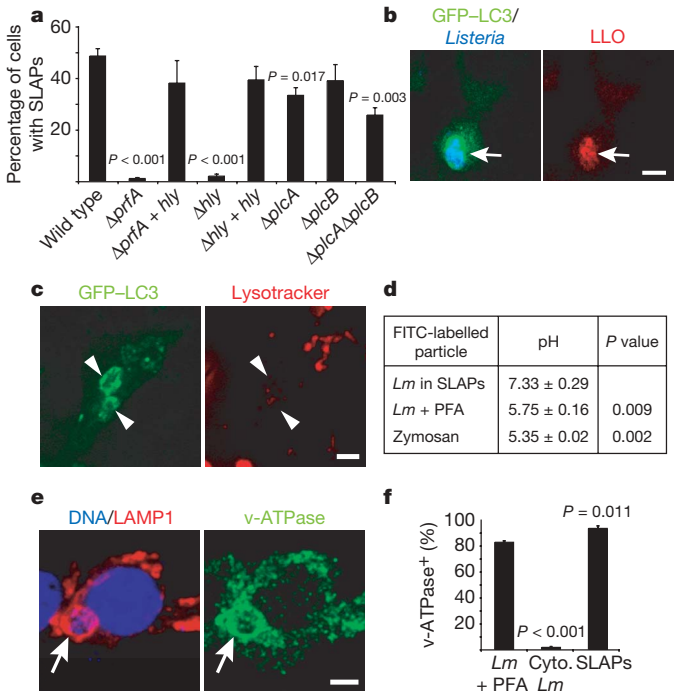

Figure 3 | SLAP formation requires bacterial LLO expression. a, GFP–LC3-transfected macrophages were infected for 4 h, and the percentage of infected cells exhibiting SLAPs was quantified. Mean ± s.e.m. for three independent experiments. *P* values for strains with significant differences from wild-type levels are shown. **b**, The arrow indicates a GFP–LC3$^+$ SLAP with internal LLO expression in cells infected for 4 h. Scale bar, 5 μm. **c**, Arrowheads indicate GFP–LC3$^+$ SLAPs devoid of Lysotracker Red in cells infected for 4 h. **d**, The pH of FITC-labelled bacteria in SLAPs, PFA-killed bacteria or zymosan particles was determined by ratiometric imaging. *P* values compared to bacteria in SLAPs are shown. **e**, The arrow indicates a LAMP1$^+$ SLAP colocalizing with v-ATPase staining in cells infected for 4 h. Scale bar, 5 μm. **f**, The percentage of v-ATPase$^+$ SLAPs was quantified as in Fig. 2c. Mean ± s.e.m. for three independent experiments. *P* values for conditions significantly different from PFA-killed bacteria are shown.

LLO might also uncouple pH gradients across SLAP membranes. Consistent with this hypothesis, most (84 ± 4.8%) SLAPs were negative for the acidotropic dye Lysotracker Red (Fig. 3c). To measure the pH of SLAPs directly, we used ratiometric imaging of bacteria prelabelled with the pH-sensitive dye fluorescein isothiocyanate (FITC)[11]. As shown in Fig. 3d and Supplementary Fig. 4, SLAPs were found to be neutral compartments (average pH 7.3 ± 0.29). Phagosomes containing PFA-killed bacteria or zymosan particles acidified to an average pH of 5.8 ± 0.16 and 5.4 ± 0.02, respectively (Fig. 3d and Supplementary Fig. 4b), consistent with previous studies of phagolysosomes[12]. However, SLAPs were positive for v-ATPase staining (Fig. 3e, f), indicating that the proton pump was present on these compartments. These results are consistent with LLO forming small pores in the SLAP membrane to uncouple the pH gradient. Acidification is known to be required for phagosome and autophagosome maturation[13,14]. Therefore, by blocking acidification of SLAPs, LLO effectively blocks fusion of this compartment with lysosomes, allowing a population of bacteria to replicate within vacuoles.

LLO expression is required for SLAP formation. However, *L. monocytogenes* within SLAPs seem to arise from a bacterial population that does not successfully escape from the primary phagosome. Therefore, bacteria within SLAPs may have reduced LLO expression or inefficient LLO activity. It has been shown previously that LLO activity is impaired by innate immune factors in activated macrophages, and is inefficient in LAMP1$^+$ compartments and alkaline environments[5,6,10,15]. Therefore, we hypothesized that experimentally reducing LLO expression would block *L. monocytogenes* entry into the cytosol but promote bacterial replication within SLAPs. To test this, we used an LLO-deficient (*hly* mutant) of *L. monocytogenes* that expresses LLO under a tightly controlled isopropyl β-D-1-thiogalactopyranoside (IPTG)-inducible promoter (iLLO)[16]. With maximal induction, the haemolytic activity of the iLLO strain is approximately 33% that of wild-type *L. monocytogenes*[16].

We compared the intracellular replication of the iLLO strain in macrophages to that of wild-type bacteria. As expected, wild-type *L. monocytogenes* exhibited rapid replication and most bacteria were LAMP1$^-$ (Fig. 4a, c). Consistent with localization in the cytosol, we observed wild-type bacteria associated with actin 'comet tails' and undergoing actin-based motility (Fig. 4a). Intracellular numbers of wild-type bacteria peaked at 12 h post infection and then declined (Fig. 4d). In contrast, the iLLO strain grew slowly in macrophages, approaching the same intracellular numbers as wild-type *L. monocytogenes* only after 48 to 72 h post infection (Fig. 4b, d). Replication of iLLO bacteria required continuous induction of LLO expression (Fig. 4d), and removal of IPTG at 12 h post infection blocked subsequent growth (data not shown). Most iLLO bacteria remained LAMP1$^+$ (Fig. 4b, c) and did not display evidence of having entered the cytosol throughout the course of infection (Supplementary Fig. 5). Therefore, LLO permits replication of *L. monocytogenes* within vacuoles when its activity is not sufficient to drive escape into the cytosol.

SLAPs were positive for the autophagy marker LC3 (Fig. 2b, c), and we have shown previously that *L. monocytogenes* can be targeted by autophagy early in infection[17]. Therefore, we hypothesized that autophagy may be involved in SLAP formation. In support of this, we found that autophagy inhibitors blocked SLAP formation (Supplementary Fig. 6). Because SLAP formation required LLO (Fig. 3a), we hypothesized that autophagy targets damaged phagosomes to prevent bacterial escape into the cytosol. To test this hypothesis, we infected autophagy-deficient (*Atg5*$^{-/-}$) mouse embryonic fibroblasts (MEFs)[18] with iLLO bacteria. On induction of LLO expression, these bacteria grew rapidly in *Atg5*$^{-/-}$ MEFs (Fig. 4e). Under these conditions, most bacteria did not colocalize with LAMP1 (Fig. 4f). In contrast, autophagy-competent MEFs maintained iLLO bacteria within LAMP1$^+$ vacuoles and delayed the kinetics of their replication (Fig. 4e, f). In the absence of induction, iLLO bacteria did not replicate in either cell type (Fig. 4e). In control

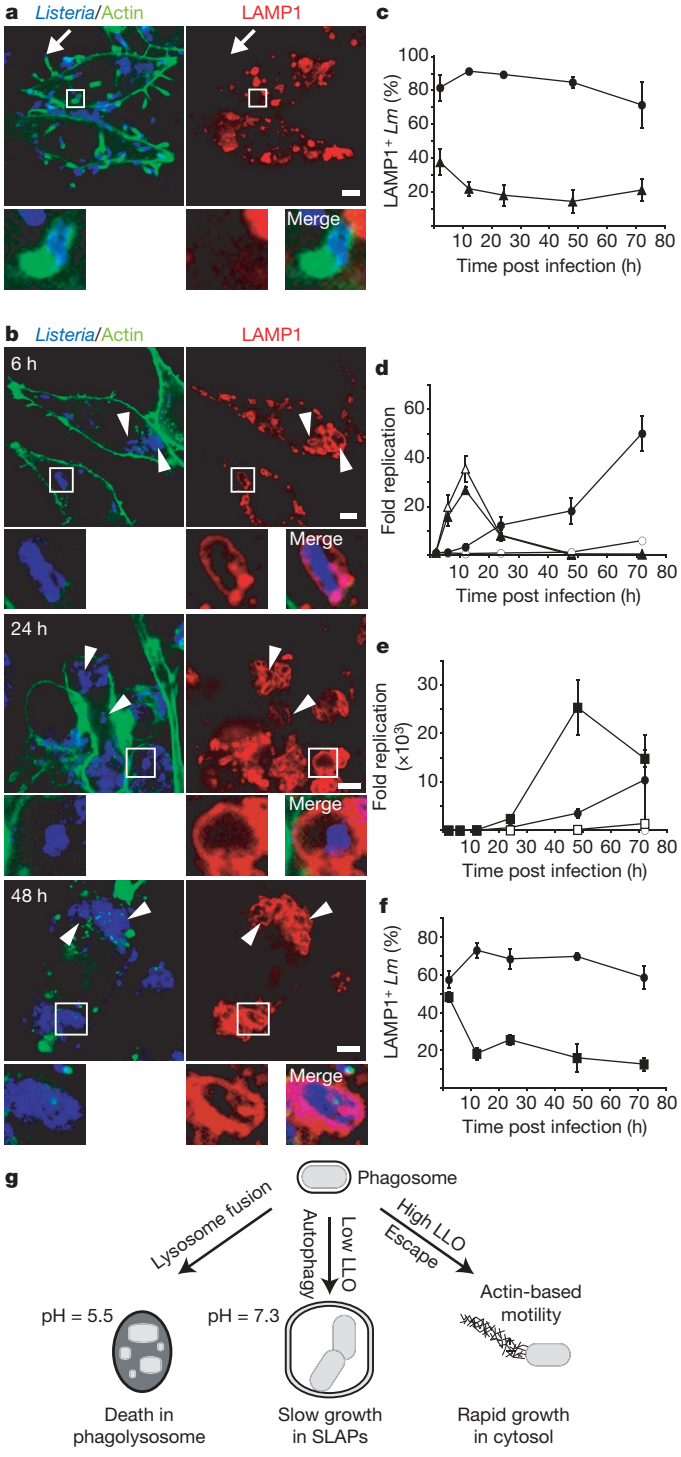

Figure 4 | Impaired LLO expression allows slow bacterial replication within vacuoles. **a**, Arrows indicate LAMP1$^-$ wild-type bacteria with actin 'comet tails' in cells infected for 6 h. The boxed region is magnified in the bottom left panels. The merged image for this region is shown at the bottom right. Scale bar, 5 μm. **b**, Macrophages were infected with IPTG-induced iLLO bacteria. Arrowheads indicate actin$^-$ iLLO bacteria within LAMP1$^+$ vacuoles. **c**, Macrophages were infected with wild-type (triangles) or IPTG-induced iLLO (circles) bacteria, and the percentage of LAMP1$^+$ bacteria was quantified. Mean ± s.e.m. for three independent experiments. **d**, Macrophages were infected as in **c** with or without IPTG induction. Intracellular bacterial replication was determined using a gentamicin-protection assay. Shown is fold replication compared to 2 h post infection. Clear triangles, wild type; filled triangles, wild type + IPTG; clear circles, iLLO; filled circles, iLLO + IPTG. Mean ± s.e.m. or range for three (wild type, wild type + IPTG, iLLO + IPTG) or two (iLLO–IPTG) independent experiments, respectively. **e**, Wild-type or *Atg5*$^{-/-}$ MEFs were infected with iLLO bacteria, and intracellular bacterial replication was determined as in **d**. Mean ± s.e.m. for three independent experiments. Clear circles, wild-type MEFs; filled circles, wild-type MEFs + IPTG; clear squares, *Atg5*$^{-/-}$ MEFs; filled squares, *Atg5*$^{-/-}$ MEFs + IPTG. **f**, Wild-type (circles) or *Atg5*$^{-/-}$ (squares) MEFs were infected as in **e** with IPTG induction. The percentage of LAMP1$^+$ bacteria was quantified as in **c**. Mean ± s.e.m. for three independent experiments. **g**, Model of the different fates of *L. monocytogenes* in host cells. High LLO activity allows bacterial escape from phagosomes. Under conditions where LLO activity is not sufficient to drive escape (low LLO), autophagy maintains bacteria within non-degradative vacuoles (SLAPs) that allow slow bacterial growth. Bacteria can also be degraded in phagolysosomes.

experiments, ~90% of wild-type bacteria were LAMP1$^-$ throughout infection in both autophagy-competent and autophagy-deficient MEFs (data not shown), demonstrating that normal LLO expression is sufficient to drive phagosomal escape in this cell type. These studies demonstrate that autophagy restricts *L. monocytogenes* replication to LAMP1$^+$ vacuoles under conditions when LLO expression is impaired.

Here we present the first study of mechanisms governing *L. monocytogenes* replication in vacuoles of host cells. We characterize a novel compartment, the SLAP, which is permissive for bacterial replication. *L. monocytogenes* replicate rapidly in the cytosol (doubling time of approximately 40 min[1,19]) but slowly within SLAPs (doubling time of approximately 8 h, Fig. 2f). It is not known whether the mechanisms governing SLAP formation *in vitro* are the same as those involved in the morphogenesis of bacteria-containing vacuoles during infection of SCID mice[2]. However, the fact that these structures both label with endocytic markers, are morphologically comparable and contain multiple bacteria suggests that the mechanisms of formation are similar.

Bacterial replication within SLAPs seems to represent a delicate balance between virulence factors of the pathogen and innate immune mechanisms of the infected cell. LLO was necessary and sufficient for *L. monocytogenes* replication within SLAPs. Therefore, LLO can be ascribed several key virulence functions: blocking nascent phagosome maturation by uncoupling the pH gradient across the phagosomal membrane[4]; mediating phagosome escape[1]; and triggering autophagy of damaged phagosomes and blocking their maturation, leading to SLAP formation and bacterial growth in vacuoles (this study). Therefore, differential LLO activities seem to give rise to different fates of *L. monocytogenes* within host cells (Fig. 4g). Our studies also demonstrate that a host cellular process, namely autophagy, maintains *L. monocytogenes* in vacuoles, particularly when LLO activity is impaired. SLAPs seem to represent a 'stalemate' for *L. monocytogenes* infection. The host cell is able to sustain viability by preventing bacterial colonization of the cytosol, but is unable to eradicate the pathogen. At the same time, the pathogen is able to replicate in SLAPs but at a reduced rate compared to that in its favoured niche, the cytosol. It remains to be seen whether other bacterial pathogens that express cholesterol-dependent cytolysins[3] utilize these toxins in a manner similar to LLO to promote their growth in vacuoles in host cells.

METHODS SUMMARY

The *L. monocytogenes* strains used are listed in Methods. Infections of C.B-17/ICR SCID mice were performed as described previously[2]. *In vitro* infections were performed in the presence of gentamicin to prevent extracellular growth at a multiplicity of infection (MOI) of 10 for RAW 264.7 macrophages and an MOI of 50 for MEFs (unless otherwise stated in Methods). LLO expression in iLLO bacteria was induced as described previously[16]. Any pharmacological agents used are listed in Methods.

TEM and immunofluorescence were performed as described[8,20,21]. Antibodies and dyes used are listed in Methods. Antigen retrieval (boiling in 10 mM sodium citrate) was performed for tissue and BrdU staining.

Most colocalization quantifications were performed by direct visualization on a Leica DMIRE2 epifluorescence microscope. All images shown are confocal *z* slices taken using a Zeiss Axiovert confocal microscope and LSM 510 software. Live imaging was performed on a Leica DMIRE2 inverted confocal microscope with a Hamamatsu Back-Thinned EM-CCD camera and spinning disk scan head. Volocity software (Improvision) was used to analyse images and to assemble *z* slices. Figure assembly was done using Adobe PhotoShop and Adobe Illustrator.

For pH measurements, wild-type bacteria, PFA-killed IgG-opsonized bacteria or zymosan particles were covalently labelled with 0.5 mg ml^{-1} FITC and added to RFP-LC3-transfected RAW 264.7 cells for 45 min or 4 h as indicated. Ratiometric imaging was performed as described previously[11] on a Leica DM IRB microscope with 485 nm and 438 nm excitation filters and a Cascade II CCD camera. Where appropriate, a corresponding red channel image (545 nm excitation) was acquired. Calibrations were performed with isotonic K^+ solutions of known pH values containing 1 μM nigericin.

The mean ± standard error (s.e.m.) is shown in figures, and *P* values were calculated using a two-tailed two-sample equal variance Student's *t*-test. A *P* value of less than 0.05 was determined to be statistically significant.

Full Methods and any associated references are available in the online version of the paper at www.nature.com/nature.

Received 25 September; accepted 13 November 2007.

1. Portnoy, D. A., Auerbuch, V. & Glomski, I. J. The cell biology of *Listeria monocytogenes* infection: the intersection of bacterial pathogenesis and cell-mediated immunity. *J. Cell Biol.* **158,** 409–414 (2002).
2. Bhardwaj, V., Kanagawa, O., Swanson, P. E. & Unanue, E. R. Chronic *Listeria* infection in SCID mice: requirements for the carrier state and the dual role of T cells in transferring protection or suppression. *J. Immunol.* **160,** 376–384 (1998).
3. Kayal, S. & Charbit, A. Listeriolysin O: a key protein of *Listeria monocytogenes* with multiple functions. *FEMS Microbiol. Rev.* **30,** 514–529 (2006).
4. Shaughnessy, L. M., Hoppe, A. D., Christensen, K. A. & Swanson, J. A. Membrane perforations inhibit lysosome fusion by altering pH and calcium in *Listeria monocytogenes* vacuoles. *Cell. Microbiol.* **8,** 781–792 (2006).
5. Myers, J. T., Tsang, A. W. & Swanson, J. A. Localized reactive oxygen and nitrogen intermediates inhibit escape of *Listeria monocytogenes* from vacuoles in activated macrophages. *J. Immunol.* **171,** 5447–5453 (2003).
6. del Cerro-Vadillo, E. *et al.* Cutting edge: a novel nonoxidative phagosomal mechanism exerted by cathepsin-D controls *Listeria monocytogenes* intracellular growth. *J. Immunol.* **176,** 1321–1325 (2006).
7. Pamer, E. G. Immune responses to *Listeria monocytogenes*. *Nature Rev. Immunol.* **4,** 812–823 (2004).
8. Perrin, A. J., Jiang, X., Birmingham, C. L., So, N. S. & Brumell, J. H. Recognition of bacteria in the cytosol of Mammalian cells by the ubiquitin system. *Curr. Biol.* **14,** 806–811 (2004).
9. Hamon, M., Bierne, H. & Cossart, P. *Listeria monocytogenes*: a multifaceted model. *Nature Rev. Microbiol.* **4,** 423–434 (2006).
10. Henry, R. *et al.* Cytolysin-dependent delay of vacuole maturation in macrophages infected with *Listeria monocytogenes*. *Cell. Microbiol.* **8,** 107–119 (2006).
11. Jankowski, A., Scott, C. C. & Grinstein, S. Determinants of the phagosomal pH in neutrophils. *J. Biol. Chem.* **277,** 6059–6066 (2002).
12. Hackam, D. J. *et al.* Regulation of phagosomal acidification. Differential targeting of Na^+/H^+ exchangers, Na^+/K^+-ATPases, and vacuolar-type H^+-ATPases. *J. Biol. Chem.* **272,** 29810–29820 (1997).
13. Gordon, A. H., Hart, P. D. & Young, M. R. Ammonia inhibits phagosome–lysosome fusion in macrophages. *Nature* **286,** 79–80 (1980).
14. Yamamoto, A. *et al.* Bafilomycin A1 prevents maturation of autophagic vacuoles by inhibiting fusion between autophagosomes and lysosomes in rat hepatoma cell line, H-4-II-E cells. *Cell Struct. Funct.* **23,** 33–42 (1998).
15. Beauregard, K. E., Lee, K. D., Collier, R. J. & Swanson, J. A. pH-dependent perforation of macrophage phagosomes by listeriolysin O from *Listeria monocytogenes*. *J. Exp. Med.* **186,** 1159–1163 (1997).
16. Alberti-Segui, C., Goeden, K. R. & Higgins, D. E. Differential function of *Listeria monocytogenes* listeriolysin O and phospholipases C in vacuolar dissolution following cell-to-cell spread. *Cell. Microbiol.* **9,** 179–195 (2007).
17. Birmingham, C. L. *et al. Listeria monocytogenes* evades killing by autophagy during colonization of host cells. *Autophagy* **3,** 442–451 (2007).
18. Kuma, A. *et al.* The role of autophagy during the early neonatal starvation period. *Nature* **432,** 1032–1036 (2004).
19. de Chastellier, C. & Berche, P. Fate of *Listeria monocytogenes* in murine macrophages: evidence for simultaneous killing and survival of intracellular bacteria. *Infect. Immun.* **62,** 543–553 (1994).
20. Brumell, J. H., Rosenberger, C. M., Gotto, G. T., Marcus, S. L. & Finlay, B. B. SifA permits survival and replication of *Salmonella typhimurium* in murine macrophages. *Cell. Microbiol.* **3,** 75–84 (2001).
21. Kaniuk, N. A. *et al.* Ubiquitinated-protein aggregates form in pancreatic beta-cells during diabetes-induced oxidative stress and are regulated by autophagy. *Diabetes* **56,** 930–939 (2007).

Supplementary Information is linked to the online version of the paper at www.nature.com/nature.

Acknowledgements J.H.B. holds an Investigators in Pathogenesis of Infectious Disease Award from the Burroughs Wellcome Fund and is the recipient of the Premier's Research Excellence Award from the Ontario Ministry of Economic Development and Trade and the Boehringer Ingelheim (Canada) Young Investigator Award in Biological Sciences. Laboratory infrastructure was provided by a New Opportunities Fund from the Canadian Foundation for Innovation and the Ontario Innovation Trust. C.L.B. holds a Canada Graduate Scholarship from the Natural Sciences and Engineering Research Council of Canada. N.A.K. holds a CAG/CIHR/Axcan Pharma fellowship from the Canadian Association of Gastroenterology. B.E.S. is supported by Canadian Institutes of Health Research and McLaughlin Centre for Molecular Medicine MD/PhD studentships. We are grateful to E. R. Unanue for performing *in vivo* infections of mice and providing tissue sections and electron micrographs. We thank D. Brown, P. Cossart, J. Danska, E. Gouin, S. Grinstein, N. Jones, N. Mizushima, D. Portnoy, and T. Yoshimori for providing reagents and suggestions. We also thank M. Woodside, P. Paroutis and R. Temkin for assistance with microscopy.

Author Information Reprints and permissions information is available at www.nature.com/reprints. Correspondence and requests for materials should be addressed to J.H.B. (john.brumell@sickkids.ca).

METHODS

***In vivo* infections.** Infections of C.B-17/ICR SCID mice were performed as described previously[2].

Cell culture and bacterial strains. RAW 264.7 macrophages and wild-type and *Atg5*$^{-/-}$ MEFs[18] were maintained in DMEM medium (HyClone) with 10% FBS (Wisent) at 37 °C in 5% CO_2 without antibiotics. Bone-marrow derived macrophages harvested from NOD mice were provided by J. Danska and maintained in supplemented growth media containing 10 ng ml^{-1} granulocyte monocyte colony stimulating factor for 6–7 days before use.

L. monocytogenes were grown in brain-heart infusion (BHI) broth and the following strains used: wild-type 10403S (ref. 22), Δ*actA* (DP-L3078, ref. 23), Δ*prfA* (DP-L4137, ref. 24), Δ*prfA* + *hly* (DH-L919, ref. 17), Δ*hly* (DP-L2161, ref. 25), Δ*hly* + *hly* (DP-L4818, ref. 26), Δ*plcA* (DP-L1552, ref. 27), Δ*plcB* (DP-L1935, ref. 28), Δ*plcA*Δ*plcB* (DP-L1936, ref. 28), iLLO (DH-L1239, ref. 16) and Δ*actA* iLLO (DH-L1257, ref. 16).

***In vitro* infections.** Most infections of macrophages were performed as described previously[17]. An MOI of 10 was used, except for Fig. 4b in which an MOI of 100 was used. Infection of macrophages with iLLO bacteria was performed as described previously[16]. Bacteria were induced with 0.5 mM IPTG for 2 h before infection, and 10 mM IPTG was maintained in the media for the duration of the experiment. For infection of MEFs with iLLO *L. monocytogenes*, bacteria were grown overnight at room temperature (~22 °C). Cells were infected as above at an MOI of 50, and gentamicin added to the media at 1 h post infection. Gentamicin-protected intracellular replication assays were performed as described previously[17]. Fold replication was determined by dividing CFUs at the desired time by CFUs at 2 h post infection. For IPTG pulse-chase experiments, macrophages were infected with IPTG-induced iLLO bacteria as above. At 12 h, cells were extensively washed with PBS, and media without IPTG was added for the remainder of the experiment.

To kill bacteria with PFA, bacteria grown overnight in BHI broth were harvested, washed in PBS and rotated at room temperature for 30 min in 13% PFA. Bacterial killing was confirmed by plating on growth plates.

Chloramphenicol (200 μg ml^{-1}) was added at 3 h post infection. Autophagy inhibitors wortmannin (Sigma; 100 nM), 3-methyladenine (Sigma; 10 mM) and LY294002 (Sigma; 100 μM) were added at 30 min post infection. Nocodazole (Sigma; 5 μM) and cytochalasin D (Sigma; 10 μM) were added at 1 h post infection.

Transmission electron microscopy, immunofluorescence and transfection. For TEM, cells were fixed in 2% glutaraldehyde overnight (~16 h) at room temperature and processed as described previously[8].

Immunofluorescence of tissue sections was performed as described previously[21] with an antigen-retrieval step (boiling in 10 mM sodium citrate buffer (pH 6.0) for 30 min). For immunofluorescence of tissue culture cells, cells were fixed with 2.5% PFA for 10 min at 37 °C, except for LLO staining (methanol at −20 °C for 10 min) and cathepsin D and v-ATPase staining (post-fix with methanol at −20 °C for 10 min). Permeabilization and blocking were performed with 0.2% saponin and 10% normal goat serum overnight at 4 °C. Staining was performed as described previously[20]. Quantifications were performed on a Leica DMIRE2 epifluorescence microscope. All images shown are confocal *z* slices from a Zeiss Axiovert confocal microscope using LSM 510 software.

The following antibodies and dyes were used: rabbit anti-*L. monocytogenes* (generated as described previously[29]), rat anti-LAMP1 (Developmental Studies Hybridoma Bank under the auspices of the NICHD and maintained by the University of Iowa), mouse anti-ubiquitinated proteins (Affiniti Research Products Ltd), mouse anti-LLO (generated as described previously[30]), rabbit anti-cathepsin D (Scripps Research Institute), rabbit anti-v-ATPase (from D. Brown) and phalloidin conjugated to AlexaFluor 488 or 568 (Molecular Probes). All secondary antibodies used were AlexaFluor conjugates (Molecular Probes). DAPI (Molecular Probes) was used according to the manufacturer's instructions.

BrdU was added to the media for 1 h and cells were fixed in methanol at −20 °C for 20 min. Antigen retrieval was performed (boiling in 10 mM sodium citrate buffer (pH 6.0) for 10 min) before samples were permeabilized/blocked in 5% BSA with 0.2% saponin. Staining was performed as above. Goat anti-BrdU was from J. Gordon.

Cells were transfected with FuGene 6 (Roche Diagnostics) or ExGen 500 (Fermentas) according to the manufacturers' instructions. GFP–LC3 and the plasmid expressing monomeric red fluorescent protein were generated as described previously[31,32].

Lysotracker labelling. Coverslips seeded with cells were maintained in imaging chambers in RPMI media with HEPES (without bicarbonate) (HyClone). Bacteria grown overnight at 37 °C shaking were diluted 1:10, subcultured for 2 h, and added to the cells at an MOI of 30. Cells were incubated at 37 °C with 5% CO_2. At 30 min, extracellular bacteria were removed by washing and gentamicin was added to the media. At 4 h, live imaging was performed on a Leica DMIRE2 inverted confocal microscope with a Hamamatsu Back-Thinned EM-CCD camera and spinning disk scan head. Volocity software (Improvision) was used. Lysotracker Red (Molecular Probes; 100 nM) was loaded into cells at the time of infection.

pH measurements. Bacteria were labelled with 0.5 mg ml^{-1} FITC in PBS (pH 8.9) for 20 min shaking at 37 °C, followed by extensive washing. For PFA-killed samples, labelled *L. monocytogenes* were treated with PFA as above and were opsonized in 10 mg ml^{-1} human IgG by rotating for 1 h at room temperature. Zymosan (Molecular Probes) particles were incubated with 0.5 mg ml^{-1} FITC and were IgG-opsonized using zymosan opsonizing reagent (Molecular Probes).

RFP–LC3-transfected RAW cells were used for all experiments. Live bacterial invasion was performed with FITC–*L. monocytogenes* as above. FITC–PFA-killed bacteria were centrifuged onto cells at 250*g* for 5 min at 4 °C. Cells were incubated at 37 °C to allow phagocytosis. At 30 min, cells were placed on ice, and goat anti-human AlexaFluor 568 (Molecular Probes) was added to the coverslip for 2.5 min to label extracellular bacteria. The antibody was washed off and cells incubated at 37 °C for a further 15 min (total of 45 min after addition of PFA-killed bacteria). FITC–zymosan were centrifuged onto cells at 550*g* for 1 min. Cells were incubated for 5 min at 37 °C to allow for particle internalization, and then vigorously washed to remove uninternalized particles. Phagosome maturation was allowed to proceed for 45 min.

Samples were maintained at 37 °C and imaged with a Leica DM IRB microscope. pH was measured by fluorescence ratiometric imaging. Light was transmitted alternately through 485 ± 10 nm and 438 ± 12 nm excitation filters and directed with a 505 nm dichroic mirror. Emitted light filtered with a 535 ± 20 nm emission filter was captured by a Cascade II CCD camera. The filter wheel and camera were controlled with Metafluor software (Molecular Devices). Where appropriate, a corresponding red channel image (545 ± 15 nm excitation filter, 570 nm dichroic mirror, and 610 ± 37 nm emission filter) was acquired to discern either extracellular PFA-killed bacteria or RFP–LC3 signal.

In situ calibrations were performed by sequentially bathing the cells in isotonic K^+ solutions (145 mM KCl, 10 mM glucose, 1 mM $MgCl_2$, 1 mM $CaCl_2$ and 20 mM of either HEPES or MES or acetate) buffered to pH values from 5.0 to 7.5 and containing 1 μM nigericin. The resulting fluorescence intensity ratio (490/440 nm) as a function of pH was fit to a Boltzmann sigmoid and was used to interpolate pH values from the experimental ratio data.

All image analysis was carried out using background-subtracted fluorescence intensities for user-defined regions-of-interest with MetaFluor software. PFA-killed-bacteria-containing phagosomes were identified by the lack of extracellular secondary antibody (red) staining. SLAPs were identified as large RFP–$LC3^+$ structures that colocalized with bacteria.

Statistics. Colocalization quantifications were performed by direct visualization on a Leica DMIRE2 epifluorescence microscope (except confocal *z* slices were used for Fig. 4c). At least 100 bacteria, cells or SLAPs were counted for each condition in each experiment. For pH measurements, 15–25 SLAPs, at least 60 PFA-killed bacteria or at least 170 zymosan particles were analysed. At least three independent experiments were performed unless otherwise indicated (two independent experiments were performed for Lysotracker studies). The mean ± s.e.m. is shown in figures unless otherwise indicated, and *P* values were calculated using a two-tailed two-sample equal variance Student's *t*-test. A *P* value of less than 0.05 was determined to be statistically significant.

22. Bishop, D. K. & Hinrichs, D. J. Adoptive transfer of immunity to *Listeria monocytogenes*. The influence of *in vitro* stimulation on lymphocyte subset requirements. *J. Immunol.* **139**, 2005–2009 (1987).
23. Skoble, J., Portnoy, D. A. & Welch, M. D. Three regions within ActA promote Arp2/3 complex-mediated actin nucleation and *Listeria monocytogenes* motility. *J. Cell Biol.* **150**, 527–538 (2000).
24. Cheng, L. W. & Portnoy, D. A. *Drosophila* S2 cells: an alternative infection model for *Listeria monocytogenes*. *Cell. Microbiol.* **5**, 875–885 (2003).
25. Jones, S. & Portnoy, D. A. Characterization of *Listeria monocytogenes* pathogenesis in a strain expressing perfringolysin O in place of listeriolysin O. *Infect. Immun.* **62**, 5608–5613 (1994).
26. Lauer, P., Chow, M. Y., Loessner, M. J., Portnoy, D. A. & Calendar, R. Construction, characterization, and use of two *Listeria monocytogenes* site-specific phage integration vectors. *J. Bacteriol.* **184**, 4177–4186 (2002).
27. Camilli, A., Tilney, L. G. & Portnoy, D. A. Dual roles of plcA in *Listeria monocytogenes* pathogenesis. *Mol. Microbiol.* **8**, 143–157 (1993).
28. Smith, G. A. *et al.* The two distinct phospholipases C of *Listeria monocytogenes* have overlapping roles in escape from a vacuole and cell-to-cell spread. *Infect. Immun.* **63**, 4231–4237 (1995).

29. Dramsi, S., Levi, S., Triller, A. & Cossart, P. Entry of *Listeria monocytogenes* into neurons occurs by cell-to-cell spread: an *in vitro* study. *Infect. Immun.* **66,** 4461–4468 (1998).
30. Nato, F. *et al.* Production and characterization of neutralizing and nonneutralizing monoclonal antibodies against listeriolysin O. *Infect. Immun.* **59,** 4641–4646 (1991).
31. Kabeya, Y. *et al.* LC3, a mammalian homologue of yeast Apg8p, is localized in autophagosome membranes after processing. *EMBO J.* **19,** 5720–5728 (2000).
32. Campbell, R. E. *et al.* A monomeric red fluorescent protein. *Proc. Natl Acad. Sci. USA* **99,** 7877–7882 (2002).